Journal of
Instrumentation

PAPER • OPEN ACCESS

Initial characterization of the ASPIRE $^{4}He^{+}$ ion beam using EBT4 radiochromic film and Monte Carlo simulation

To cite this article: N. Clements *et al* 2026 *JINST* **21** P04007

Published by IOP Publishing for Sissa Medialab

Received: *December 19, 2025*
Revised: *March 4, 2026*
Accepted: *March 22, 2026*
Published: *April 14, 2026*

Initial characterization of the ASPIRE $^4He^+$ ion beam using EBT4 radiochromic film and Monte Carlo simulation

N. Clements,[a,*] **L. Dufort-Gagnon**,[a] **A. Irving-Hughes**,[b] **E. Yuan**,[b] **M. Michielan**,[c] **O. Masella**,[a] **H. Klassen**,[d,e] **C.R.J. Charles**[e,f] **and M. Bazalova-Carter**[a]

[a] *Department of Physics and Astronomy, University of Victoria, 3800 Finnerty Rd, Victoria, BC, V8P 5C2, Canada*
[b] *Department of Chemistry, University of British Columbia, 2036 Main Mall, Vancouver, BC, V6T 1Z1, Canada*
[c] *Department of Physics, University of Trento, Via Sommarive, 14, 38123 Povo TN, Italy*
[d] *Department of Mathematics, University of Toronto, 40 St George St, Toronto, ON, M5S 3H4, Canada*
[e] *TRIUMF, 4004 Wesbrook Mall, Vancouver, BC, V6T 2A3, Canada*
[f] *Department of Chemistry, Simon Fraser University, 8888 University Drive, Burnaby, BC, V5A 1S6, Canada*

E-mail: nclements@uvic.ca

Abstract: Experimental radiochromic film dosimetry of a helium-4 ion beam at subclinical energies (0.5–1.5 MeV/u) was performed at the newly commissioned ASPIRE facility at TRIUMF. Peeled GafChromic EBT4 films were irradiated with low-energy $^4He^+$ ions, then scanned and analyzed to assess their suitability for spatial and quantitative dosimetry at these energies. To account for the film under-response caused by the high linear energy transfer (LET) of the beam, a correction factor was applied based on the mean LET calculated across the film's active layer using simulations. Monte Carlo simulations were performed with TOPAS to model dose deposition in the EBT4 film. Agreement between film measurements and Monte Carlo results was variable, largely limited by the lack of accurate delivered beam charge measurements. The experiments also revealed beam asymmetries and smaller-than-expected beam widths, attributed to suboptimal tuning of the accelerator chain. Overall, peeled EBT4 films were shown to be a practical tool for spatial beam characterization of helium-ion beams at subclinical energies. However, large uncertainties in delivered beam charge and measured doses beyond the range of EBT4 and the calibration curve used made accurate dosimetry impossible. This work motivates future studies at higher, more clinically relevant energies, where improved charge measurement and beam stability will be critical.

Keywords: Dosimetry concepts and apparatus; Ion sources (positive ions, negative ions, electron cyclotron resonance (ECR), electron beam (EBIS)); Models and simulations; Instrumentation for heavy-ion therapy

*Corresponding author.

https://doi.org/10.1088/1748-0221/21/04/P04007

Contents

1 Introduction

Today, approximately half of all cancer patients are prescribed radiation therapy as part of their treatment [1, 2]. The majority of radiation therapy patients will receive treatment with photon beams [3]. Even though the number of proton and ion therapy facilities has greatly increased over the last few decades [4], less than 1% of cancer patients are treated with protons or ions due to the high treatment facility cost.

Proton and heavier ion beams are attractive sources in radiotherapy because of their distinct depth-dose behaviour. A monoenergetic ion beam produces a sharp peak known as the Bragg peak at a specific depth (depending on energy and the medium), enabling high dose delivery to the tumour while keeping entrance dose low and minimizing exit dose [5].

In recent years, interest in ^{4}He and other ions has been revived since neither protons nor carbon ions have proven to be the ideal radiotherapy particle type, and ^{4}He ions present a reasonable compromise between the benefits and drawbacks of each. In 2021, the Heidelberg Ion Beam Therapy Center (HIT) treated a patient with ^{4}He ions for the first time since the last treatment at the Lawrence Berkeley National Lab in 1992 [6]. The Heavy Ion Medical Accelerator in Chiba (HIMAC) is a Japan-based accelerator that can perform ^{4}He ion treatment either as a standalone particle or integrated in a multi-ion therapy program [7, 8].

Although current clinical helium therapy employs beams with energies of several hundred MeV/u, this work is an initial exploratory study investigating the dosimetric properties of an up to 1.5 MeV/u $^{4}He^{+}$ ion beam using radiochromic film measurements and Monte Carlo (MC) simulations. Here, the feasibility of $^{4}He^{+}$ ion beam dosimetry at subclinical energies accelerated at the newly commissioned ASPIRE facility of TRIUMF is explored to motivate further research at higher beam energies.

Radiochromic films are useful dosimeters in research in both X-ray imaging [9–11] and radiation therapy [12–14]. GafChromic EBT4 film (Ashland Inc, Bridgewater, NJ), benefits from a high spatial resolution (~ 25 µm), near-tissue equivalence, and a dynamic dose range (0.2–10 Gy), and does not require post-exposure treatment [15, 16]. EBT GafChromic films have been used for dosimetry of a wide variety of sources including monochromatic 25–35 keV synchrotron x-ray beams [17], polychromatic 20–220 kVp beams generated by x-ray tubes [18, 19], 6–25 MV photon beams and [20–22], 4–15 MeV electron beams [23, 24], 63–230 MeV proton beams [25, 26], 50–200 MeV very-high energy electron (VHEE) beams [27–30], and many more.

A few groups have used EBT GafChromic films as dosimeters for alpha particle emitting radionuclides. In particular, Diaz-Martinez et al. developed a dose calibration protocol for Am-241 using unlaminated EBT3 film and MC simulations [31], Ng et al. proposed a method for producing and verifying the integrity of peeled EBT3 films and demonstrated that calibration curves for peeled and unpeeled films were essentially equivalent [32], and Mukherjee et al. proposed peeled EBT3 films for activity calibration of alpha emitting radionuclides [33]. These studies have found that unlaminated/peeled EBT film is an effective dosimeter for alpha particles.

Two works have previously performed radiochromic film dosimetry on ^{4}He ion beams. Torrisi et al. investigated the response of HD-810 GafChromic film to ^{4}He ions and compared the normalized optical absorbance at 673 nm to the ^{4}He ion absorbed dose [34]. They found that for ^{4}He ions at 600 keV, the response was linear for doses lower than approximately 250 Gy. Grilj et al. assessed the LET-dependence of unlaminated EBT3 and MD-V3 using various ion sources [35]. For EBT3, film response decreased with LET and was found to have more than a 50% underresponse at an LET of 100 keV/µm for a 9 MeV ^{4}He beam.

The goal of this work was to perform radiochromic film dosimetry of an accelerated $^4He^+$ beam at ASPIRE to evaluate and characterize the behaviour and tune characteristics of the beam through the accelerator at different energies.

2 Materials and methods

2.1 ASPIRE and TRIUMF overview

The AStrochemical and Planetary materials IRradiation Experiment (ASPIRE) is a newly commissioned experimental facility in the medium energy beam transport (MEBT) section of the ISAC (Isotope Separator and ACcelerator) complex of TRIUMF in Vancouver, BC, Canada [36]. Positive ion beams of isotopes from nearly all chemical elements are created for ISAC experiments like ASPIRE at the Off-Line Ion Sources (OLIS) facility using surface, microwave, and Electron-Cyclotron Resonance (ECR) ion sources. This study uses $^4He^+$ produced only by the OLIS microwave ion source at a potential of 8.16 kV and accelerated up to 1.5 MeV/u at the present MEBT location of ASPIRE [36]. Figure 1(a) and 1(b) shows the highly customizable irradiation vacuum chamber of ASPIRE, where film samples for irradiation were mounted to custom multi-position sample wheels, rotatable by a precision stepper motor system via a Raspberry Pi EPICS (Experimental Physics and Industrial Control System) interface.

2.2 Experimental setup

For this experiment, accelerated $^4He^+$ ions were used at energies of 0.5, 1.0, and 1.5 MeV/u to irradiate EBT4 radiochromic films. Since $^4He^+$ ions at these energies cannot penetrate through the 125 µm polyester layer to reach the active layer of EBT4 film, the top polyester layer of the EBT4 film was

2026 JINST 21 P04007

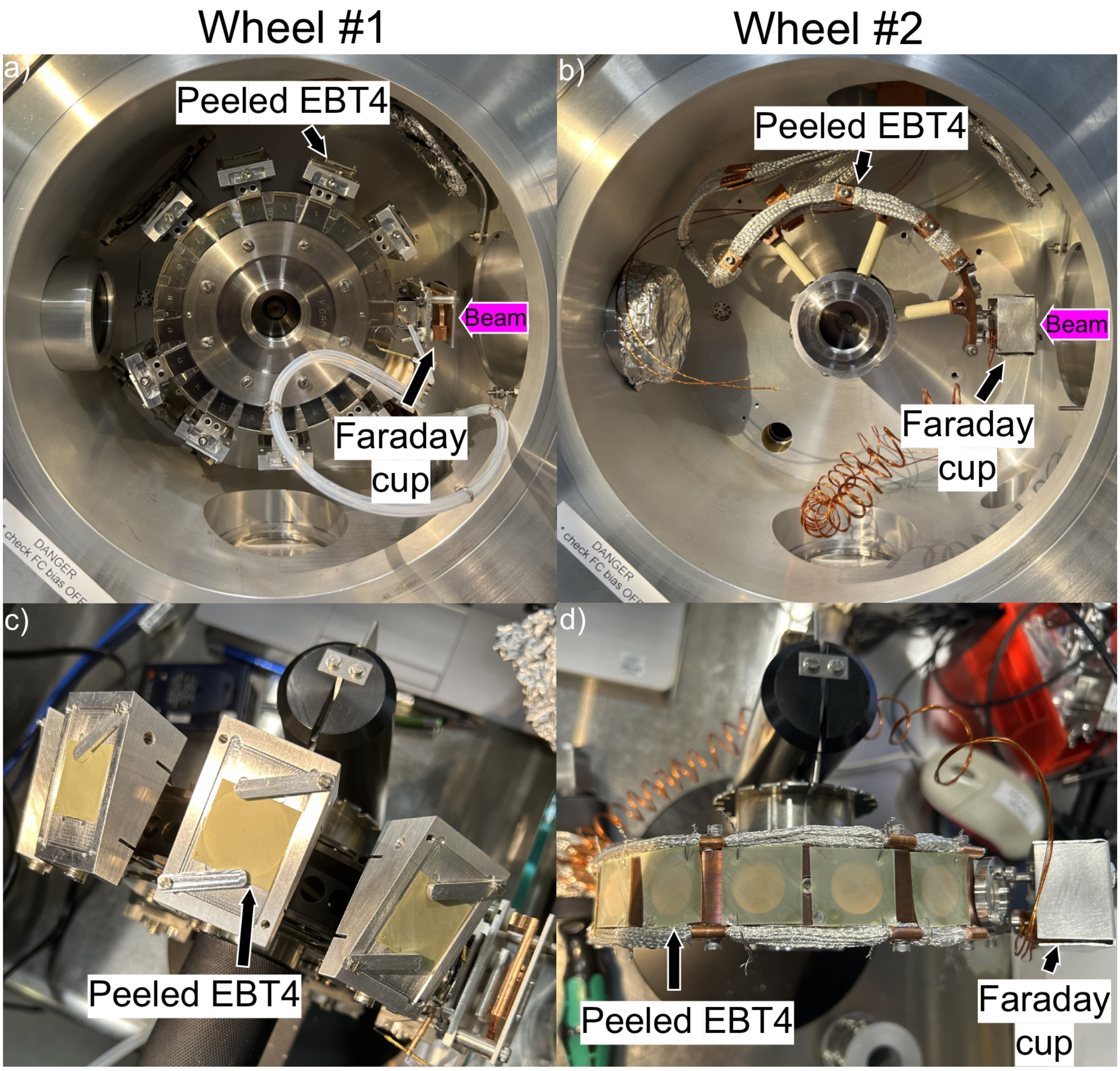

Figure 1. a) The first experimental ASPIRE wheel with holders clamping down peeled EBT4 films. b) The second experimental ASPIRE wheel with peeled EBT4 films attached by tying them onto the wheel using stainless steel wire, which pierced the films. c) and d) the respective wheels in the experimental vacuum chamber for irradiation.

peeled off. The peeling process was performed using a scalpel to separate the top layer at a corner and then peel it off, attempting to minimize active layer removal and damage, similar to previous publications [33, 37]. The structure of EBT4 film before and after peeling is shown in figure 2.

For all irradiations, the targeted $^4He^+$ ion beam size was a full-width at half-maximum (FWHM) of 10 mm, and the desired beam charge delivered was 10 pC (~ 62.4 million particles), which was expected to result in doses that would be within the usable dose range of EBT4 film based on preliminary MC simulations. To achieve 10 pC of delivered beam charge, a beam current of 10 pA was targeted using attenuators at the OLIS ion source, and one-second irradiations were performed. Attenuating the ion source to low current increases the inherent sensitivity of the accelerator chain to fluctuations in current. Although beam current was measured before ASPIRE on a Faraday Cup

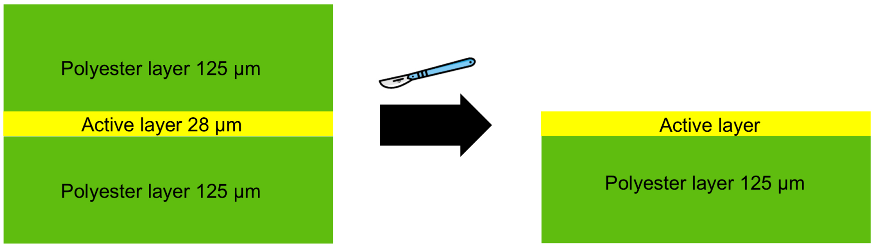

Figure 2. The structure of GafChromic EBT4 film before and after peeling off one of the polyester base layers.

~ 30 cm upstream from the vacuum chamber on the MEBT beamline, the desired 10 pA current was at the low sensitivity limit for the cup and electrometer and did show large current fluctuations.

Film irradiations were performed with two different sample wheels, as shown in figure 1. For all irradiations, films were cut into $2.54 \times 2.54\,\text{cm}^2$ pieces. For the first wheel, eight peeled EBT4 films were placed onto holders at 15° on a rotating wheel, clamped down, and each film was irradiated with 1.5 MeV/u $^4He^+$ ions, targeting 10 pC of charged particles delivered (see figures 1(a) & 1(c)). For the second wheel, two sets of irradiations were performed. Seven peeled EBT4 films were tied using thin stainless steel wire, which pierced the film at two corners, and the films were approximately perpendicular to the beam (see figures 1(b) & 1(d)). For the first set, each film was irradiated with a 1.0 MeV/u $^4He^+$ ion beam, and the second set was irradiated with 0.5 MeV/u $^4He^+$ ions, targeting 10 pC each time.

2.3 Film analysis

All $^4He^+$ ion irradiated films were scanned 24 hours post-irradiation at 300 dpi and with a 48-bit color depth using an Expression 10000 XL scanner (Epson, Suwa, Japan). The red channel was used for film analysis since it is the most sensitive colour channel [38], and films were analyzed using a custom Python script. Net optical density per pixel (netOD(i, j)) was calculated with a background correction as:

$$\text{netOD}(i, j) = \log_{10}\left(\frac{I_0}{I(i, j)}\right) \tag{2.1}$$

where $I(i, j)$ is the pixelwise red channel intensity of an irradiated peeled film, and I_0 is the average red channel intensity across a region of interest spanning an unirradiated peeled EBT4 film. An average was taken rather than performing this pixelwise because the peeling process introduced streaking artifacts, which varied film-to-film. Although flood-field scans were acquired, the correction factor cancels when a scalar background is used; therefore, the $netOD$ effectively represents a background-normalized measurement without pixelwise flood correction. Considering the flood scan, the standard deviation as a percentage of the mean pixel value was 0.65% across the analyzed ROI, so residual spatial variation was considered minimal.

Dose to water from film was then calculated from the background-corrected optical density using:

$$D_{\text{water}} = \frac{(a \cdot \text{netOD})}{(c - \text{netOD})} \cdot \text{RE}(E) \tag{2.2}$$

where D_{water} is the dose-to-water from $^4He^+$ ions, netOD is the net optical density, and a and c are curve fit parameters from a calibration curve that was done with a 225 kVp x-ray spectrum for

2026 JINST 21 P04007

this batch of EBT4 film. The calibration data and the fitted curve are shown in figure 3. The fitted curve was $D = (a \cdot \text{netOD})/(c - \text{netOD})$ and the coefficient of determination was $R^2 = 0.9997$. The calibration was performed in solid water at 2 cm depth using a Farmer ionization chamber (PTW TN30010-1) following TG-61 protocol with at least 5 cm of solid water for backscatter [39]. The Comet MXR-225/26 x-ray tube from the KOALA system [40] was used and operated at 225 kVp with 2 mm of Al filtration.

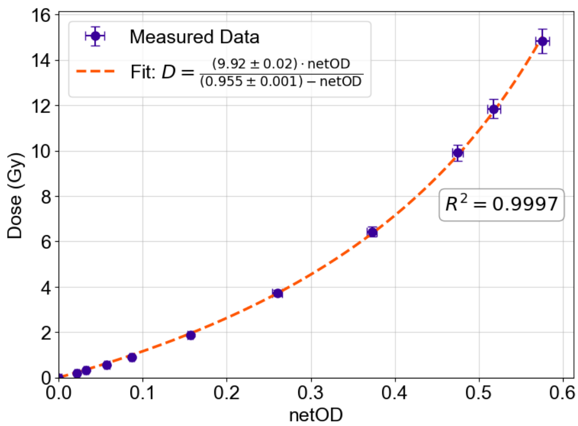

Figure 3. Calibration curve for EBT4 film created for a 225 kVp x-ray beam.

Lastly, the $\text{RE}(E)$ parameter of equation 2.2 is the relative effectiveness, which accounts for the underresponse of the EBT4 film to high LET radiation. To calculate this parameter, the mean LET across the active layer was calculated for each beam energy. This was done by simulating a 1 cm × 1 cm, flat, square beam incident on a 1 cm × 1 cm × 28 µm active layer of EBT4 in TOPAS Monte Carlo. The active layer composition was based on the work of Palmer et al. with EBT3, since EBT4 was unchanged in atomic composition from its predecessor (see table 1). The energy deposited was scored in the active layer, which was split into a 1 × 1 × 50 scoring grid. For each of the 0.5, 1.0, and 1.5 MeV/u beams, 10^6 $^4He^+$ particles were simulated, and the LET for each voxel was calculated as the mean energy deposited per particle divided by the length of each voxel along the beam direction.

The mean LET was calculated by averaging all non-zero voxels for each of the 1.5, 1.0, and 0.5 MeV/u energies across the length of the active layer. From the work of Grilj et al. [35], $\text{RE}(E)$ was then calculated using an empirical equation:

$$\text{RE}(E) = \frac{45}{0.49 \cdot \overline{\text{LET}}(E) + 45} \tag{2.3}$$

where $\overline{\text{LET}}(E)$ is the mean LET in the active layer for the $^4He^+$ beam at a given energy. This expression was derived empirically by Grilj et al. by fitting measured EBT3 film dose-response data with a bimolecular saturation model and observing that the half-saturation dose $D_{1/2}$ increases approximately linearly with LET. The relative effectiveness was then defined as the ratio of the low-LET (250 kVp x-ray-equivalent) $D_{1/2}$ to the LET-dependent $D_{1/2}$, yielding the functional form in equation 2.3.

For each energy, films that contain most of the beam without significant artifacts were chosen for data analysis. Three films were analyzed for 1.5 MeV/u, two for 1.0 MeV/u, and all seven for 0.5 MeV/u. For these films, a 2D Gaussian fit was performed on beam profiles to determine the beam size and the peak dose for each irradiation.

2026 JINST 21 P04007

Table 1. Thickness, density, and mass percent composition of EBT4 film from Palmer et al. [41].

EBT4 layer	Thickness (μm)	Density (g/cm^3)	Mass composition (%)				
			H	Li	C	O	Al
Polyester base	125	1.35	4.2		62.5	33.3	
Active layer	28	1.20	8.8	0.6	51.1	32.8	6.7

2.4 Monte Carlo simulations of experimental $^4He^+$ ion irradiations

All Monte Carlo simulations were performed using TOPAS MC v3.9 [42, 43]. For all simulations, a custom physics list was used to ensure that $^4He^+$ ion interactions were accurately modelled. The seven physics modules were: `g4em-standard_opt4`, `g4radioactivedecay`, `g4decay`, `g4h-elastic_HP`, `g4h-phy_QGSP_BIC_HP`, `g4ion`, and `g4stopping`. All other physics parameters were left as their default. Simulations were run on the Digital Research Alliance of Canada's NARVAL computer cluster.

Experimental $^4He^+$ beam delivery at 0.5, 1.0, and 1.5 MeV/u was simulated using MC. For each energy, the beam was simulated using the mean beam size across films for that energy. The dose was calculated in the active layer of EBT4 film for a total delivered beam charge of 10 pC. To achieve high statistics, 10^7 histories were run for each simulation, and dose-to-medium was scored in a 300 × 300 × 1 voxel grid in the 2.54 cm × 2.54 cm × 28 μm active layer to match the voxel size to the 300 dpi scanned films. For the 1.5 MeV/u simulation, the simulated film was tilted at 15° to match the experimental setup. The composition of the active layer and base layer of the films was as shown in table 1 based on the work of Palmer et al. [41].

The active layer thickness was not measured due to its micron-level thickness and fragility. To compare film measurements and simulations while accounting for the possibility that the film active layer is thinner than 28 μm (due to peeling or manufacturing uncertainty), the average Gaussian fit to the film data for each energy was calculated assuming two possible active layer thicknesses of 28 μm and 14 μm. The difference in doses arises from the calculated mean LET through the active layer and the corresponding RE factor from equation 2.3. Similarly, the MC simulations for each energy were performed assuming both 28 μm and 14 μm active layers to reflect the potential variation in experimental film thickness.

3 Results

3.1 Film analysis

LET-depth profiles are shown in figure 4. For a 28-μm active layer, the mean LET values for the 1.5, 1.0, and 0.5 MeV/u $^4He^+$ beams were 115, 166, and 188 keV/μm, respectively. These corresponded to RE values of 0.443, 0.356, and 0.328, calculated using equation 2.3. Dose-to-water was then obtained using equation 2.2.

Measured 2D film dose maps and Gaussian fits provided beam profiles for all irradiations at 1.5, 1.0, and 0.5 MeV/u. Table 2 summarizes the fitted FWHM values and peak doses.

2026 JINST 21 P04007

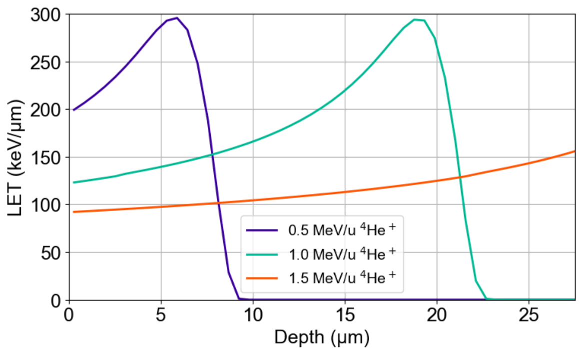

Figure 4. Linear Energy Transfer (LET) through the active layer of EBT4 for 0.5, 1.0, 1.5 MeV/u $^4He^+$ beams.

Representative 2D dose distributions from three irradiations at 1.5 MeV/u using wheel #1 are shown in figure 5(a)–(c), with the corresponding x- and y-profiles in figures 5(d)–(g). The fitted FWHM values and peak doses are listed in table 2. The beam width in the y-direction was 12 mm on average, approximately 20% larger than the intended 10 mm. The x-direction width was 2.6 mm, corresponding to a 74% reduction relative to the nominal 10 mm width. The mean peak dose from the Gaussian fits was (45.8 ± 13.6) Gy.

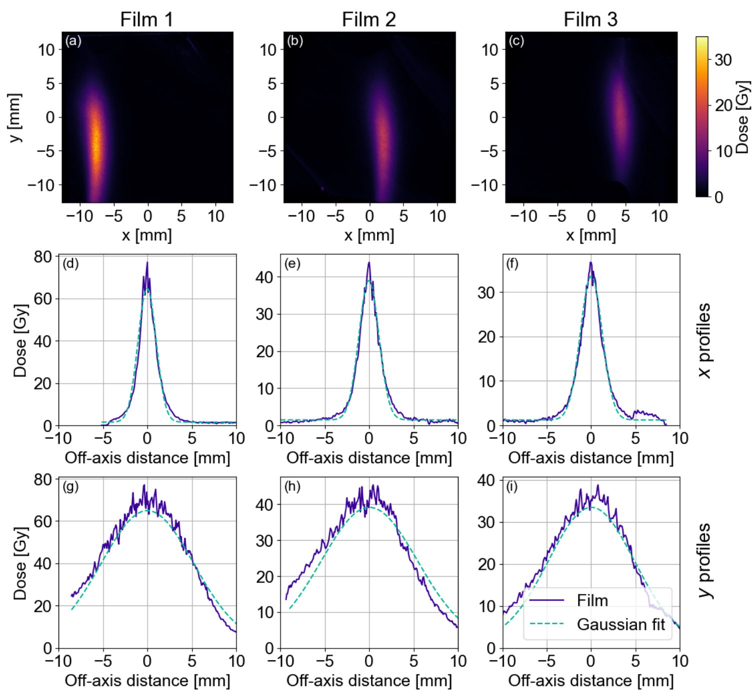

Figure 5. (a)–(c) 2D dose distributions from EBT4 film from 1.5 MeV/u $^4He^+$ ions. (d)–(i) 1D dose profiles with the Gaussian fit to the film shown as a dashed cyan line.

Figure 6(a)–(b) shows 2D dose maps from two irradiations using wheel #2. The corresponding profiles are shown in figures 6(c)–(f). FWHM and peak dose values are given in table 2. The average beam width in y was 12.7 mm, 27% larger than intended, while the x-direction width was 2.5 mm, 75% smaller than the nominal value. The mean peak dose was (29.2 ± 0.4) Gy.

2026 JINST 21 P04007

Table 2. Measured beam size and peak dose for $^4He^+$ ion beams at 1.5, 1.0, and 0.5 MeV/u measured using peeled EBT4 film.

Energy	Sample	FWHM$_x$ [mm]	FWHM$_y$ [mm]	Peak Dose [Gy]
1.5 MeV/u	Film 1	2.24	11.94	64.8
	Film 2	2.64	12.82	39.0
	Film 3	2.83	11.79	33.5
	Mean ± SD	2.57 ± 0.30	12.18 ± 0.52	45.8 ± 13.6
1.0 MeV/u	Film 1	2.43	13.67	28.8
	Film 2	2.57	11.70	29.5
	Mean ± SD	2.50 ± 0.07	12.69 ± 0.99	29.2 ± 0.4
0.5 MeV/u	Film 1	5.58	4.28	164.4
	Film 2	5.98	4.59	113.9
	Film 3	5.08	4.09	186.0
	Film 4	5.58	4.48	83.3
	Film 5	5.08	4.19	154.9
	Film 6	5.18	3.88	204.9
	Film 7	5.89	4.87	75.5
	Mean ± SD	5.48 ± 0.34	4.34 ± 0.33	140.4 ± 46.6

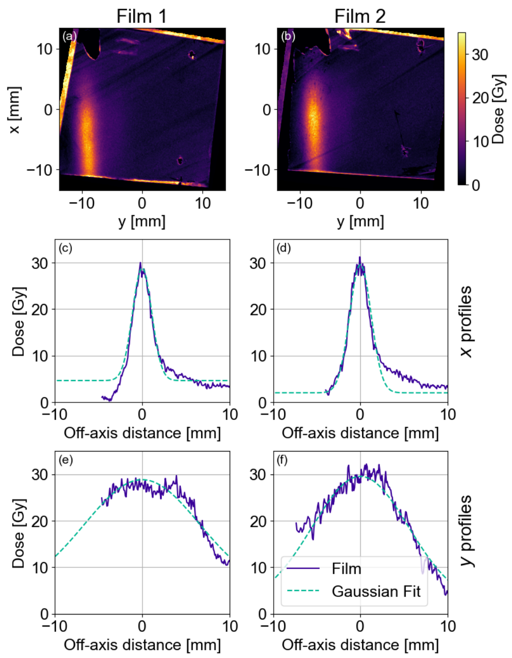

Figure 6. (a) & (b) 2D dose distributions from EBT4 film from 1.0 MeV/u $^4He^+$ ions. (c)–(f) 1D dose profiles with the Gaussian fit to the film shown as a dashed cyan line.

Figure 7 shows 2D dose distributions for all seven irradiations at 0.5 MeV/u, with corresponding 1D profile fits. Table 2 lists the FWHM values and peak doses.

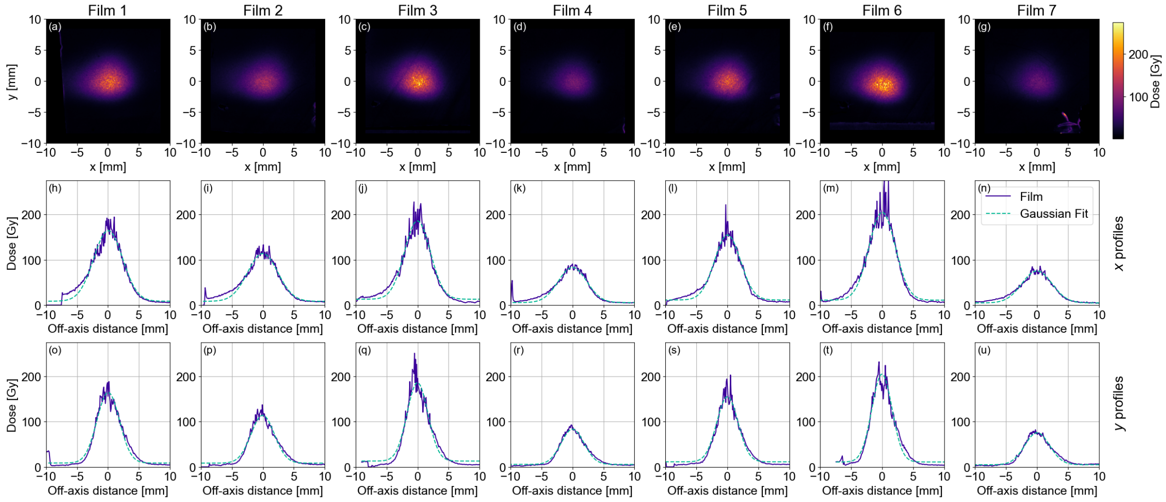

Figure 7. (a)–(g) 2D dose distributions from EBT4 film from 0.5 MeV/u $^4He^+$ ions. (h)–(u) 1D dose profiles with the Gaussian fit to the film shown as a dashed cyan line.

The beam shape was more symmetric at this energy. The average FWHM values were 4.3 mm in x and 5.5 mm in y, corresponding to reductions of 57% and 45% relative to the intended 10 mm width. The mean peak dose was (140.4 ± 46.6) Gy.

3.2 Monte Carlo simulations of experimental $^4He^+$ ion irradiations

The mean LET ($\overline{LET}$) and relative effectiveness (RE) values for 1.5, 1.0, and 0.5 MeV/u, calculated for 14 µm and 28 µm active layer thicknesses, are shown in table 3. These values were derived from figure 4 and equation 2.3, respectively. The mean peak dose across the analyzed films is also presented, together with the corresponding MC peak dose and their percent difference.

Table 3. Mean LET and RE for 0.5, 1.0, and 1.5 MeV/u $^4He^+$ ions for 14 µm and 28 µm active layers. Comparison of peak doses from experiment using EBT4 film and Monte Carlo simulations for each energy and active layer thickness.

Energy [MeV/u]	EBT4 active layer thickness [µm]	$\overline{LET}$ [keV/µm]	RE	Mean peak dose (film) [Gy]	Peak dose (MC) [Gy]	% difference
1.5	14	100	0.478	42.3	25.0	+69%
	28	115	0.443	45.6	29.3	+56%
1.0	14	153	0.375	27.7	36.2	−24%
	28	166	0.356	29.2	33.7	−13%
0.5	14	188	0.328	140	45.3	+209%
	28	188	0.328	140	22.4	+525%

4 Discussion

This work presents, to the authors' knowledge, the first experimental radiochromic film dosimetry of an accelerated $^4He^+$ ion beam at subclinical energies of 0.5–1.5 MeV/u. Peeled EBT4 films were successfully scanned and analyzed following irradiation on the newly commissioned ASPIRE facility at TRIUMF.

For all $^4He^+$ ion irradiations, the aim was a beam size of 10 mm (FWHM). As seen in table 2, the beam size varied greatly. For both 1.5 MeV/u and 1.0 MeV/u, the beam size in the y-direction was 2–3 millimetres larger than the intended size; however, in the x-direction, it appeared to be ~ 4× smaller than intended. This change in shape of the beam is due to an asymmetric tune of the beam through the MEBT section of the accelerator to the last Faraday Cup before the ASPIRE chamber. That cup, being the last diagnostic before the chamber, provides no spatial information on the beam (only current intensity) and, until this study, beam shape as a function of accelerator tune was never quantifiable at ASPIRE. For the 0.5 MeV/u irradiations, the beam was more symmetric, with the mean FWHM in the x-direction being 5.48 mm and 4.34 mm in the y-direction. However, the beam size was much smaller than the intended 10 mm FWHM due to the same inability to spatially quantify the spatially asymmetric beam tune through MEBT at this different energy. Due to the smaller beam sizes, the peak doses were much higher than intended and previously calculated by MC. The high dose regions were well outside of the film calibration curve and the recommended dose level for EBT4. While the Gaussian shape of the beam provided some confidence that the high-dose measurements are plausible, the dose points above 15 Gy exhibit high noise. These differences highlight the critical need to implement a precision XY beam imaging system at ASPIRE to ensure spatially symmetric tunes prior to sample irradiations.

When $^4He^+$ ions fully stop within the film active layer, the average absorbed dose becomes highly sensitive to the layer thickness due to the steep dose gradients along the particle range. For example, 1.0 MeV/u and 0.5 MeV/u $^4He^+$ ions exhibit Bragg peaks at depths of approximately 6 µm and 19 µm, respectively (figure 9). Peeling of the polyester base layer in EBT4 films can remove a portion of the active layer as well, effectively reducing the volume in which the dose is measured. Because absorbed dose is defined as energy deposited per unit mass, modelling the active layer as thicker than it truly is can significantly distort the calculated dose and contribute to discrepancies between film measurements and MC simulations (figure 8).

Figure 9 shows the depth-dose profiles for the three beam energies used in this study for both a 28 µm water layer and the EBT4 active layer. These profiles demonstrate not only that a thinner active layer alters the measured dose, but also that the EBT4 active layer cannot be treated as water-equivalent at these energies, as seen by the differences in the profiles. The impact of active-layer thickness on both the MC calculations (through the conversion of deposited energy to dose using the modelled mass of the scoring volume) and the film measurements (through changes in the mean LET across the layer and the resulting variations in relative effectiveness) is illustrated by the shaded regions in figure 8.

The LET-depth profiles shown in figure 4 were used to calculate the mean LET in the active layer for each beam. For the initial film analysis, the mean LET was taken as the average of all non-zero LETs up to 28 µm depth. This resulted in mean LET values of 115, 166, and 188 keV/µm, which were used to calculate the RE factor for equation 2.3. The RE correction was based on the work of Grilj et al., which found good agreement from 0 to 100 keV/µm [35]. However, since the mean LETs of this work were higher than the range considered in that study, some scrutiny is warranted.

Many films were excluded from the analysis due to significant artifacts arising from both the peeling process and the mounting method. In several cases, the small tabs used to clamp the films (figure 1(c)) obstructed a substantial portion of the beam. Additionally, some films from wheel #2 exhibited artifacts

2026 JINST 21 P04007

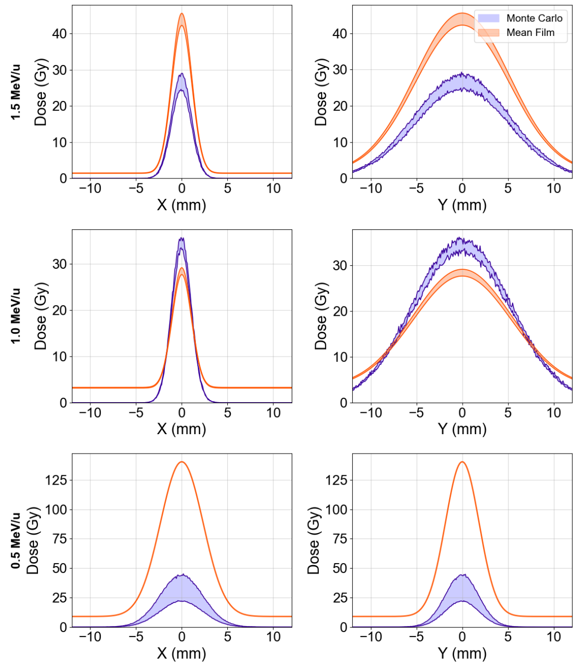

Figure 8. D dose profiles from the mean Gaussian fit to EBT4 film data and Monte Carlo at 1.5, 1.0, and 0.5 MeV/u. The shaded region represents the difference in doses seen from a 14 μm active layer to a 28 μm active layer.

around the piercing location, which in certain cases extended into the beam profile. Overall, these issues encourage developing an alternative method for mounting films in vacuum for future experiments.

Considering the film analysis, the 1D profiles and 2D dose distributions in figures 5, 6, and 7, showed that the beam profiles were relatively Gaussian, given the accuracy of the Gaussian fits to the data. Noise is seen throughout the profiles, likely due to streaking artifacts from the peeling process — which are best seen in figure 6(a) and 6(b). Noise also appears to be worsened at higher doses; this is clearly seen in the 0.5 MeV/u profiles of figure 7.

For the 1.5 MeV/u $^4He^+$ ion irradiations, the beam size in the y-direction was approximately 12 mm; however, in the x-direction, it was only 2.5 mm. In terms of film dose compared to simulation, the mean peak dose to film was 69% higher than MC for a 28 μm active layer and 56% higher for a 14 μm active layer. This was likely due to more beam charge delivered than intended due to beam current fluctuations.

For the 1.0 MeV/u $^4He^+$ ion irradiations, the beam size was smaller than intended in the x-direction, similar to 1.5 MeV/u. The mean peak dose to film was 13% lower than MC for a 28 μm active layer and 24% lower for a 14 μm active layer. The higher doses seen in MC are likely due to the delivered beam charge to the film being less than 10 pC.

For the 0.5 MeV/u $^4He^+$ ion irradiations, the beam was much more symmetric (see figure 7 and table 2); however, imperfections are still seen in the beam shape and are most evident in the 2D distributions shown in figures 7(a)–(g). The mean beam size was $(\text{FWHM}_x, \text{FWHM}_y) = (5.48 \pm 0.34, 4.34 \pm 0.33)$ and was still smaller than the expected 10 mm FWHM. Overall, the mean peak dose on film was 525% higher than MC for a 28 μm active layer and 209% higher than MC for a 14 μm active layer. The much higher doses suggest much greater than 10 pC was delivered to the films and the large difference between peak doses between the 14 μm and 28 μm active layers can be attributed to how shallow the Bragg peak occurs in the active layer (∼ 6 μm).

2026 JINST 21 P04007

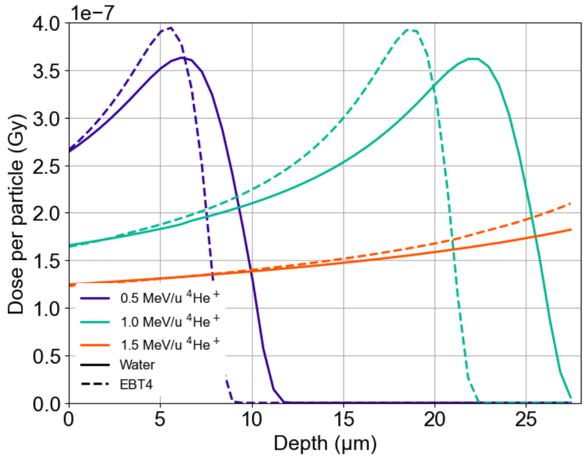

Figure 9. Depth dose curves for 0.5, 1.0, and 1.5 MeV/u $^4He^+$ beams in water and in the active layer of EBT4.

The dominant uncertainties in this work were on the delivered beam charge, the accuracy of netOD-to-dose conversion for measured doses greater than 15 Gy, and the active layer thickness. The intended delivered beam charge for each irradiation was ~ 10 pC of $^4He^+$. However, due to the present limitations of the MEBT beamline and diagnostics at ASPIRE, accurate beam charge measurement was not possible. Although beam current was monitored using a Faraday cup upstream of the vacuum chamber, 5–10 pA represented the lower limit of stable cup operation due to the existing amplifier system in use. Furthermore, irradiation to the vacuum chamber was manually triggered, introducing an additional source of uncertainty. Consequently, the delivered beam charge may have been considerably higher or lower than the nominal 10 pC. A conservative estimate is that the current could have fluctuated down to half or up to twice the intended value, and that the 1s shot was 1 ± 0.5 s, resulting in a delivered beam charge $Q \in [2.5, 30]$ pC.

Measured doses were up to 205 Gy, significantly greater than the recommended dose range for EBT4 film and the highest dose used for film calibration (15 Gy). While the high-dose regions of the film profiles are noisy (see figure 7), the overall Gaussian-like shape offers some confidence in the Gaussian fits performed to the data. Nevertheless, extrapolation of the calibration curve was necessary for doses > 15 Gy and should therefore be interpreted primarily qualitatively.

Finally, uncertainty in the active layer thickness can considerably impact the measured doses, particularly for 0.5 MeV/u (see table 3). The active layer thickness was not measured due to its micron-level thickness and fragility. However, to consider a possible range of thicknesses, dose deposition in active layer thicknesses of 28 µm and 14 µm was simulated using Monte Carlo methods.

Other sources of uncertainty include the use of equation 2.3 to estimate the relative effectiveness (RE) values from the mean LET across the active layer for LETs up to 188 keV/µm, despite the equation having been derived using data with maximum mean LET values of 100 keV/µm.

To quantify the potential impact of this extrapolation, a sensitivity analysis was performed in which the strength of the LET dependence in equation 2.3 was varied by a conservative ±25%. For the highest LET case considered in this work (188 keV/µm), this yielded RE values between 0.281 and 0.394, corresponding to a maximum systematic uncertainty of 20% in the RE value. For LET values of 166 keV/µm and 115 keV/µm, the resulting dose uncertainties were approximately 19% and 15%, respectively.

Although extrapolation of the RE model introduces a systematic uncertainty of up to ~ 20%, this contribution remains small compared to the much larger uncertainties associated with delivered beam charge and extrapolation of the film calibration curve at high doses. Finally, the Monte Carlo statistical uncertainties on all calculated quantities were less than 1%.

In summary, the large uncertainty in the delivered beam charge and the required extrapolation of the netOD-to-dose calibration above 15 Gy are the primary contributors to the discrepancies observed between Monte Carlo simulations and film measurements.

These experiments represent early ion beam work on the newly commissioned ASPIRE facility at TRIUMF. Radiochromic film dosimetry was performed for $^4He^+$ ions with energies ranging from 0.5 to 1.5 MeV/u, and the measurements were compared with MC simulations. Peeled EBT4 films proved to be a useful tool for spatial beam characterization of low-energy $^4He^+$ ions. However, accurate determination of the delivered beam charge per irradiation is critical for dosimetric assessment and comparison with MC simulations. Measurement of the film active layer after the peeling process could also prove informative. Future experiments would most benefit from reproducible beam size and beam charge delivery, higher energies to improve clinical relevance, and an air- rather than vacuum-based irradiation setup using solid water slabs.

5 Conclusions

This work demonstrates that peeled EBT4 radiochromic film can provide useful spatial information for $^4He^+$ ion beams at subclinical energies of 0.5–1.5 MeV/u delivered with the ASPIRE and MEBT beamline at TRIUMF. Large uncertainties in the delivered beam charge and doses exceeding both the recommended range for EBT4 film and the applied calibration curve rendered accurate dosimetry unfeasible and prevented agreement with Monte Carlo results. Future work will focus on reproducible beam delivery, accurate beam charge measurement, including developing improved beam diagnostics and a precision trigger-shutter for irradiations, and experiments at higher, clinically relevant helium ion beam energies.

Acknowledgments

This work was funded in part by three NSERC Discovery grants (RGPIN-2021-03516, RGPIN-2022-04684, and SAPIN-2022-00026), NSERC CGRS D, an NSERC USRA and by the Canada Research Chairs program. This research was enabled in part by support provided by the BC DRI Group, Calcul Québec (www.calculquebec.ca), and the Digital Research Alliance of Canada (www.alliancecan.ca). Thank you to Dr. Ilsa Cooke of UBC for sharing beam time that enabled this work, and to B. Minato and M. Lovera of TRIUMF for machining and electromechanical help.

References

[1] Y. Lievens, J.M. Borras and C. Grau, *Provision and use of radiotherapy in Europe*, *Mol. Oncol.* **14** (2020) 1461.

[2] R. Baskar, K.A. Lee, R. Yeo and K.-W. Yeoh, *Cancer and Radiation Therapy: Current Advances and Future Directions*, *Int. J. Med. Sci.* **9** (2012) 193.

[3] R. Mohan, *A review of proton therapy — Current status and future directions*, *Precis. Radiat. Oncol.* **6** (2022) 164.

[4] S. Rossi, *Hadron Therapy Achievements and Challenges: The CNAO Experience*, *Physics* **4** (2022) 229.

[5] D. Schulz-Ertner and H. Tsujii, *Particle Radiation Therapy Using Proton and Heavier Ion Beams*, *J. Clin. Oncol.* **25** (2007) 953.

[6] RaySearch Laboratories, *Heidelberg ion beam therapy center treats first patient using helium ion therapy with raystation*, https://www.raysearchlabs.com/media/press-releases/2021/heidelberg-ion-beam-therapy-center-treats-first-patient-using-helium-ion-therapy-with-raystation/.

[7] Y. Iwata et al., *Design of a compact superconducting accelerator for advanced heavy-ion therapy*, Nucl. Instrum. Meth. A **1053** (2023) 168312.

[8] K. Katagiri et al., *First test of a newly developed 14-GHz multi-ion ECRIS*, Nucl. Instrum. Meth. A **1079** (2025) 170615.

[9] O. Rampado et al., *Radiochromic films for dental CT dosimetry: A feasibility study*, Phys. Med. **30** (2014) 18.

[10] S. Brady, T. Yoshizumi, G. Toncheva and D. Frush, *Implementation of radiochromic film dosimetry protocol for volumetric dose assessments to various organs during diagnostic CT procedures*, Med. Phys. **37** (2010) 4782.

[11] J. Boivin et al., *Reference dosimetry during diagnostic CT examination using XR-QA radiochromic film model*, Med. Phys. **38** (2011) 5119.

[12] A. Niroomand-Rad et al., *Report of AAPM Task Group 235 Radiochromic Film Dosimetry: An Update to TG-55*, Med. Phys. **47** (2020) 5986.

[13] M.J. Butson, P.K.N. Yu, T. Cheung and P. Metcalfe, *Radiochromic film for medical radiation dosimetry*, Mater. Sci. Eng. R: Rep. **41** (2003) 61.

[14] O.A. Zeidan et al., *Characterization and use of EBT radiochromic film for IMRT dose verification*, Med. Phys. **33** (2006) 4064.

[15] *Gafchromic EBT4 dosimetry film — brochure*, https://www.ashland.com/industries/medical/radiotherapy-films/ebt4.

[16] M.F. Chan, J. Park, R. Aydin and S.B. Lim, *Technical note: Energy dependence of the Gafchromic EBT4 film: Dose-response curves for 70 kV, 6 MV, 6 MV FFF, 10 MV FFF, and 15 MV x-ray beams*, Med. Phys. **50** (2023) 3738.

[17] T.A.D. Brown et al., *Dose-response curve of EBT, EBT2, and EBT3 radiochromic films to synchrotron-produced monochromatic x-ray beams*, Med. Phys. **39** (2012) 7412.

[18] J.L.G. Massillon and I.D. Muñoz-Molina and P. Díaz-Aguirre, *Optimum absorbed dose versus energy response of Gafchromic EBT2 and EBT3 films exposed to 20–160 kV x-rays and ^{60}Co gamma*, Biomed. Phys. Eng. Express **2** (2016) 045005.

[19] E. Prentou et al., *On the use of EBT3 film for relative dosimetry of kilovoltage X ray beams*, Phys. Med. **74** (2020) 56.

[20] S. Khachonkham et al., *Characteristic of EBT-XD and EBT3 radiochromic film dosimetry for photon and proton beams*, Phys. Med. Biol. **63** (2018) 065007.

[21] M. Fuss, E. Sturtewagen, C.D. Wagter and D. Georg, *Dosimetric characterization of GafChromic EBT film and its implication on film dosimetry quality assurance*, Phys. Med. Biol. **52** (2007) 4211.

[22] H. Bilge, A. Cakir, M. Okutan and H. Acar, *Surface dose measurements with GafChromic EBT film for 6 and 18 MV photon beams*, Phys. Med. **25** (2009) 101.

[23] M. Jaccard et al., *High dose-per-pulse electron beam dosimetry: Usability and dose-rate independence of EBT3 Gafchromic films*, Med. Phys. **44** (2017) 725.

[24] S. Mutsakanyi and F. du Plessis, *Characterization and dosimetry of photon multileaf collimated electron beams using Gafchromic film measurements*, Radiat. Phys. Chem. **182** (2021) 109266.

2026 JINST 21 P04007

[25] R. Castriconi et al., *Dose-response of EBT3 radiochromic films to proton and carbon ion clinical beams*, *Phys. Med. Biol.* **62** (2016) 377.

[26] D. Villoing et al., *Technical note: Proton beam dosimetry at ultra-high dose rates (FLASH): Evaluation of GAFchromic™ (EBT3, EBT-XD) and OrthoChromic (OC-1) film performances*, *Med. Phys.* **49** (2022) 2732.

[27] A. Subiel et al., *Dosimetry of very high energy electrons (VHEE) for radiotherapy applications: using radiochromic film measurements and Monte Carlo simulations*, *Phys. Med. Biol.* **59** (2014) 5811.

[28] D. Poppinga et al., *VHEE beam dosimetry at CERN Linear Electron Accelerator for Research under ultra-high dose rate conditions*, *Biomed. Phys. Eng. Express* **7** (2020) 015012.

[29] N. Clements et al., *Mini-GRID radiotherapy on the CLEAR very-high-energy electron beamline: collimator optimization, film dosimetry, and Monte Carlo simulations*, *Phys. Med. Biol.* **69** (2024) 055003.

[30] M. Bazalova-Carter et al., *Comparison of film measurements and Monte Carlo simulations of dose delivered with very high-energy electron beams in a polystyrene phantom*, *Med. Phys.* **42** (2015) 1606.

[31] V.D. Diaz-Martinez et al., *Investigation of dosimetric characteristics of radiochromic film in response to alpha particles emitted from Americium-241*, *Med. Phys.* **51** (2024) 6305.

[32] C.Y.P. Ng, S.L. Chun and K.N. Yu, *Quality assurance of alpha-particle dosimetry using peeled-off Gafchromic EBT3® film*, *Radiat. Phys. Chem.* **125** (2016) 176.

[33] B. Mukherjee et al., *A unique alpha dosimetry technique using Gafchromic EBT3textregistered film and feasibility study for an activity calibrator for alpha-emitting radiopharmaceuticals*, *Br. J. Radiol.* **88** (2015) 20150035.

[34] A. Torrisi et al., *Linearity studies of HD-810 dosimeters by light ion beams*, *Radiat. Eff. Def. Solids* **175** (2020) 383.

[35] V. Grilj and D.J. Brenner, *LET dependent response of GafChromic films investigated with MeV ion beams*, *Phys. Med. Biol.* **63** (2018) 245021.

[36] C. Charles, H. Klassen, A. Pearson, B. Haertel, E. Enkelmann, E. Yuan et al., *The astrochemical and planetary materials irradiation experiment (ASPIRE) at TRIUMF*, in the proceedings of the *56th Lunar and Planetary Science Conference*, The Woodlands, TX, U.S.A., March 10–14 (2025), paper 2098.

[37] A.S. Mustaqim, S. Kandaiya, N.N.A. Razak and N.Z. Yahaya, *The Gafchromic EBT3® film as alpha detector*, *J. Phys. Conf. Ser.* **1083** (2018) 012019.

[38] Y. Akino et al., *Correction of lateral response artifacts from flatbed scanners for dual-channel radiochromic film dosimetry*, *Journal of Radiat. Res.* **62** (2021) 319.

[39] C.M. Ma et al., *AAPM protocol for 40–300 kV x-ray beam dosimetry in radiotherapy and radiobiology*, *Med. Phys.* **28** (2001) 868.

[40] O. Masella et al., *Initial characterization of a novel dual-robot orthovoltage radiotherapy system*, *Biomed. Phys. Eng. Express* **11** (2025) 025057.

[41] A.L. Palmer, A. Dimitriadis, A. Nisbet and C.H. Clark, *Evaluation of Gafchromic EBT-XD film, with comparison to EBT3 film, and application in high dose radiotherapy verification*, *Phys. Med. Biol.* **60** (2015) 8741.

[42] B. Faddegon et al., *The TOPAS tool for particle simulation, a Monte Carlo simulation tool for physics, biology and clinical research*, *Phys. Med.* **72** (2020) 114.

[43] J. Perl et al., *TOPAS: An innovative proton Monte Carlo platform for research and clinical applications*, *Med. Phys.* **39** (2012) 6818.